SLAC–PUB–7707
November 1997

An Internally Reflecting Cherenkov Detector (DIRC): Properties of the Fused Silica Radiators [1]

I. Adam,[a] R. Aleksan,[b] D. Aston,[a] P. Bailly,[c] C. Beigbeder,[d] M. Benayoun,[c] M. Benkebil,[d] G. Bonneaud,[e] D. Breton,[d] H. Briand,[c] D. Brown,[f] Ph. Bourgeois,[b] J. Chauveau,[c] R. Cizeron,[d] J. Cohen-Tanugi,[a] M. Convery,[a, 2] P. David,[c] C. de la Vaissiere,[c] A. de Lesquen,[b] L. del Buono,[c] G. Fouque,[e] A. Gaidot,[b] F. Gastaldi,[e] J.-F. Genat,[c] L. Gosset,[b] D. Hale,[g] G. Hamel de Monchenault,[b,f] O. Hamon,[c] R. Kadel[f] J. Kadyk[f] M. Karolak,[b] H. Kawahara,[a] H. Krueger,[a] H. Lebbolo,[c] P.H. Leruste,[c] F. Le Diberder,[c] G. London,[b] M. Long,[f] J. Lory,[c,†] A. Lu,[g] A.-M. Lutz,[d] G. Lynch,[f] M. McCulloch,[a] D. McShurley,[a] R. Malchow,[h] P. Matricon,[e] B. Mayer,[b] B. Meadows,[i] J.-L. Narjoux,[c] J.-M. Noppe,[d] D. Oshatz,[f] G. Oxoby,[a] R. Plano,[j] S. Plaszczynski,[d] M. Pripstein,[f] J. Rasson,[f] B. Ratcliff,[a] R. Reif,[a] C. Renard,[e] L. Roos,[c] E. Roussot,[e] X. Sarazin,[a] M.-H. Schune,[d] J. Schwiening,[a] S. Sen,[d] V. Shelkov,[f] M. Sokoloff,[i] H. Staengle,[h] P. Stiles,[a] R. Stone,[f] Ch. Thiebaux,[e] K. Truong,[d] W. Toki,[h] G. Vasileiadis,[e] G. Vasseur,[b] J. Va'vra,[a] M. Verderi,[e] S. Versille,[c] D. Warner,[h] T. Weber,[a] T. F. Weber,[f] W. Wenzel,[f] R. Wilson,[h] G. Wormser,[d] Ch. Yéche,[b] S. Yellin,[g] B. Zhang,[c,‡] M. Zito.[b]

[a] Stanford Linear Accelerator Center, Stanford, CA 94309, USA. [b] CEA, DAPNIA, CE-Saclay, F-91191, Gif-sur-Yvette Cedex, France. [c] LPNHE des Universités Paris 6 et Paris 7, Tour 33, Bc 200, 4 Place Jussieu, F-75252, Paris, Cedex 05, France. [d] LAL Orsay, Universite Paris Sud, Batiment 200, F-91405 Orsay Cedex, France. [e] LPNHE de l'Ecole Polytechnique, Route de Saclay, F-91128 Palaiseau Cedex, France. [f] Lawrence Berkeley National Laboratory, One Cyclotron Road, Berkeley, CA 94720, USA. [g] Dept. of Physics, University of California, Santa Barbara, CA 93106, USA. [h] Dept. of Physics, Colorado State University, Fort Collins, CO 80523, USA. [i] Dept. of Physics, University of Cincinnati, Cincinnati, OH 45221, USA. [j] Dept. of Physics, Rutgers University, P.O. Box 849, Piscataway, NJ 08855, USA. [†] Retired. [‡] Permanent address: Inst. of High Energy Physics, Chinese Academy of Sciences; P.O. Box 918, Beijing 100039, The People's Republic of China.

Abstract

The DIRC, a new type of ring-imaging Cherenkov detector that images internally reflected Cherenkov light, is being constructed as the main hadronic particle identification component of the BABAR detector at SLAC. The device makes use of 5 meter long fused silica (colloquially called quartz) bars, which serve both as the Cherenkov radiators and as light pipes for transmitting the light to an array of photo-multiplier tubes. This paper describes a program of research and development aimed at determining whether bars that meet the stringent requirements of the DIRC can be obtained from commercial sources. The results of studies of bulk absorption of fused silica, surface finish, radiation damage and bulk inhomogeneities are discussed.

[1] Work supported by Department of Energy contract DE–AC03–76SF00515.

[2] Speaker and contact: Mark Convery, Stanford Linear Accelerator Center, Stanford, CA 94309, USA.

Poster presented at the 1997 IEEE Nuclear Science Symposium and Medical Imaging Conference, Albuquerque, New Mexico, USA, November 9-15 1997

I. INTRODUCTION

A key requirement for experiments studying CP-violation in B-mesons, such as BABAR at SLAC [1], is hadronic particle identification. π/K separation is needed over the full kinematic range (up to 4.0 GeV/c) to provide flavor-tagging and to aid in the analysis of rare decays. The DIRC (Detection of Internally Reflected Cherenkov Light) [2] has been selected to perform this function for BABAR. The implementation of DIRC in BABAR and the performance of several prototypes has been described elsewhere [3]. Here, we briefly describe the basic operating principles in order to motivate the studies of fused silica described here.

Figure 1 is a schematic of the DIRC principle. A fraction of the Cherenkov light emitted by a charged particle as it crosses the 17 mm thick bar is trapped by total internal reflection inside the bar. As the light propagates down the precisely rectangular bar, its angular information is retained, up to up/down and left/right ambiguities. At the end of the bar, the light is allowed to expand in a "stand-off" region and a ring-like image is formed on the detector surface. There, the light is detected by an array of photo-multiplier tubes, which are sensitive to photons between 300 and 600 nm. The radius of the ring

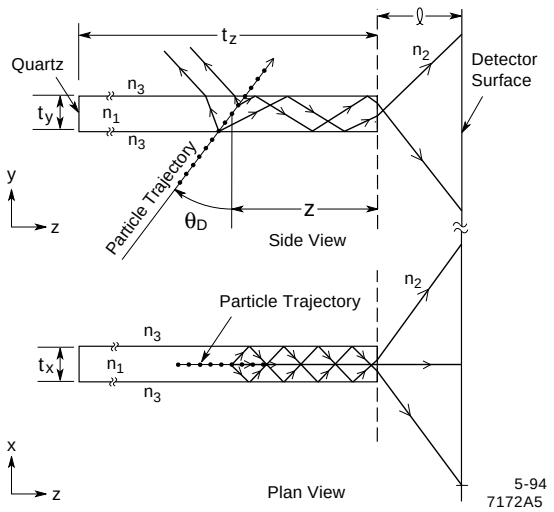

Fig. 1 Schematic of the DIRC principle shown in a single fused silica bar. The particle trajectory and representative trajectories of Cherenkov photons are shown.

gives the Cherenkov angle, which is related to the the particle velocity through

$$\cos\theta_C = \frac{1}{\beta n}, \tag{1}$$

where $\beta = v/c$ is the ratio of the particle velocity (v) to the velocity of light (c), and n is the index of refraction of the fused silica ($n \approx 1.474$). For a given momentum, particles of different mass will have different Cherenkov angles. For the benchmark case of π/K separation at $p = 4.0$ GeV/c, the difference in θ_C is 6.5 mr. The precision with which this angle may be measured depends on dip-angle. Figure 2 shows the expected π/K separation (in standard deviations) as a function of dip-angle and momentum.

In order to achieve this separation, the trapped light must be transmitted with very low losses. This places stringent requirements on the optical quality of the bars: they must reflect the trapped light with extremely high efficiency and the fused silica material must not scatter or absorb the light. A series of studies have been performed to verify that these qualities are achievable. Some of these studies can only be performed using finished fused silica bars, whereas others can most easily be done using the raw fused silica material before it is cut into bars.

II. STUDIES OF FINISHED FUSED SILICA RADIATOR BARS

Fused silica bars for use in the DIRC are manufactured to the following specifications: length $1225.0^{+0.0}_{-0.5}$mm, width $35.0^{+0.0}_{-0.5}$mm, thickness $17.2^{+0.0}_{-0.4}$mm. Four of these "short" bars, which are as long as conventional optical manufacturing techniques allow, are glued together to form one 5 meter bar.

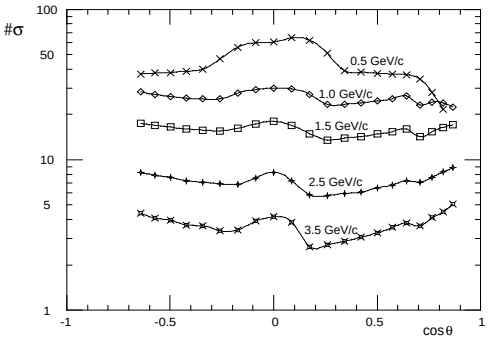

Fig. 2 Expected π/K separation for the completed DIRC.

A. Reflectivity Measurement

Since the trapped Cherenkov light must typically reflect $\approx$ 100 times before exiting the bar and being detected, the internal reflectivity coefficient of the bar surfaces must be very close to 1. A reflectivity coefficient of less than 0.999 would result in unacceptable light losses. In order to qualify the bars, then, losses as small as 10^{-4} per bounce must be measured. Such small losses are difficult to measure in a single bounce, but may be measured if a laser beam is sent down the bar at such an angle that it is totally internally reflected and bounces many times ($\approx$ 50) before exiting the bar. Figure 3 shows a bar under test with a beam reflecting down its length.

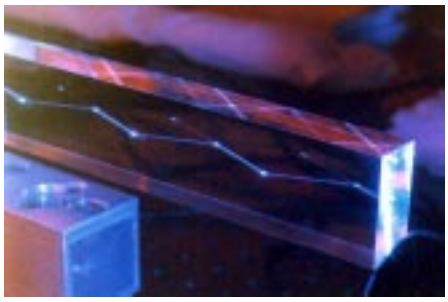

Fig. 3 Photograph of a bar undergoing the reflectivity measurement. The HeCd laser beam can be seen propagating down the bar.

For most incident angles and polarizations, the beam is split into reflected and transmitted components at the fused silica/air interfaces. Measurement of the intensities of each of these beam components as it exits the bar allows one to extract the reflectivity coefficient. This "Calorimetric" method has been used to measure the reflection coefficient of a number of prototype bars [4] [5].

The measurement can be simplified, however, if the beam is horizontally polarized and enters the bar at the Brewster angle. In that case, almost no reflected beam is produced at either fused silica/air interface, thereby simplifying the calculation of the reflection coefficient. The effect of the small amount of light that is reflected at the fused silica/air interface, which is due to imperfect laser polarization, is small and can be calibrated out. It is also desirable to scan the beam through

a number of positions in the bar in order to determine the "average" reflectivity coefficient of a significant part of the surface of the bar.

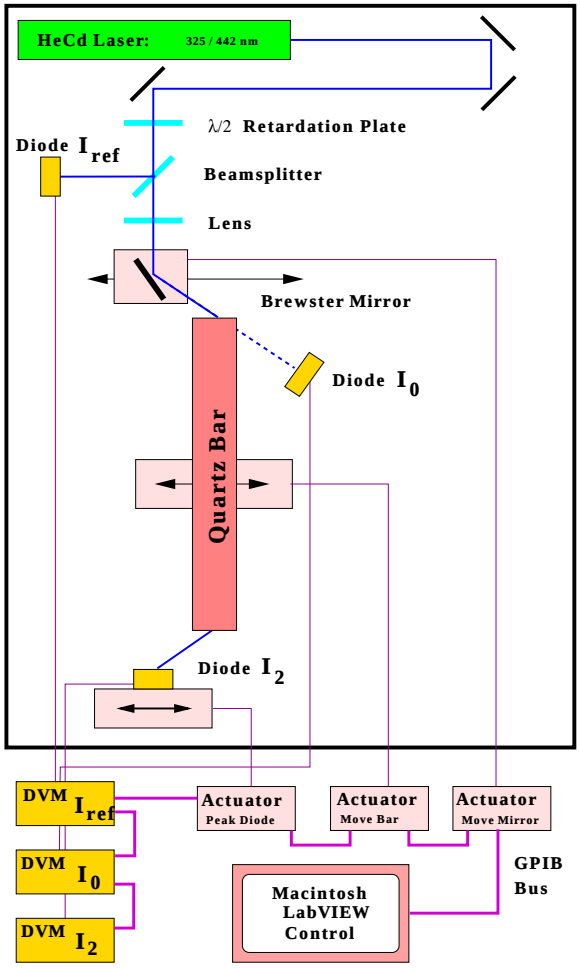

Fig. 4 Schematic of the optical scanning system used for fused silica bar quality control.

Figure 4 shows a schematic of the setup that has been used to perform this measurement [6]. A HeCd laser provides a vertically polarized laser beam with a wavelength of 442 nm that is rotated to the desired polarization with a $\lambda/2$ retardation plate. The beam then enters the bar under test, which can be scanned through the beam using an actuator under the control of a Macintosh running LabVIEW software. A number of "pre-production" bars manufactured by Zygo Corporation [7] from Heraeus Suprasil material [8] have been tested in this setup [9]. Figure 5 shows the measured average reflectivity of these bars, indicating that they are acceptable for use in the DIRC. The average reflectivity was 0.9996 ± 0.0001.

B. Bulk Transmission

A precise measurement of the bulk transmission is also performed in a similar setup. Beams with wavelengths of 442 nm and 325 nm are sent directly down the axis of the beam and

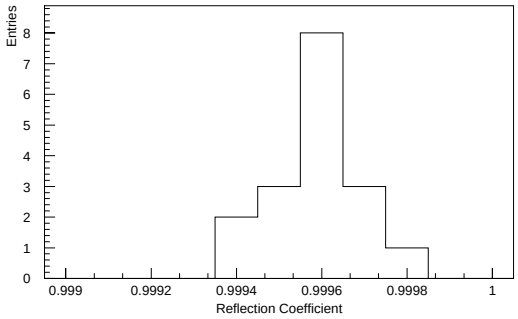

Fig. 5 Measured average reflectivity at $\lambda = 442$nm of several fused silica bars made from Heraeus Suprasil material.

the fraction of light transmitted is measured, after correcting for Fresnel reflection. Figure 6 shows the measured transmission for these bars. The average transmission was found to be (99.9 $\pm$ 0.1) %/m at 442 nm and (98.9 $\pm$ 0.2) %/m at 325 nm.

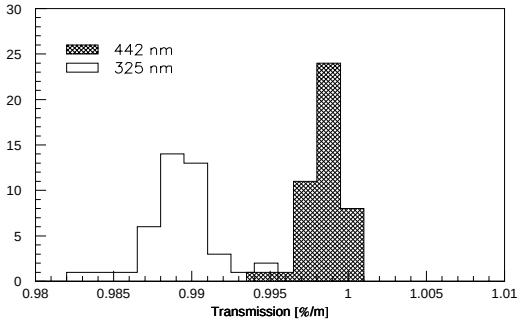

Fig. 6 Measured average transmission at two different wavelengths of several fused silica bars made from Heraeus Suprasil material.

C. Radiation Damage Tests

A further requirement on bars to be used in the DIRC is that they not lose transmission upon exposure to $\approx$ 10 krad of radiation. To verify radiation hardness, the transmission of samples of several types of fused silica was measured before and after exposure to few MeV photons from a Co^{60} source.

Seven types of fused silica were studied [11]. Three of these were types of "natural" fused silica, while four were synthetic fused silica. Natural fused silica is formed from powdered natural quartz while the synthetic fused silica is formed by flame hydrolysis of Silicon-bearing compounds, such as $SiCl_4$. Within these categories, the differences between the types have to do with proprietary manufacturing methods and starting materials.

In all cases, the natural types were found to be insufficiently radiation hard — they showed unacceptable transmission losses after $\approx$ 10krad exposure. In contrast, the synthetic types all showed little or no radiation damage even at much higher doses and were deemed acceptable for use in the DIRC. Figure 7 shows the effect of radiation damage on a sample of natural fused silica. Table 1 summarizes the results of

the radiation damage study. Based on these findings, and other considerations, Heraeus Suprasil Standard and [8] TSL Spectrosil 2000 [10] were identified as the two preferred types of fused silica for the DIRC. The rest of the studies described will involve one or both of these types of fused silica.

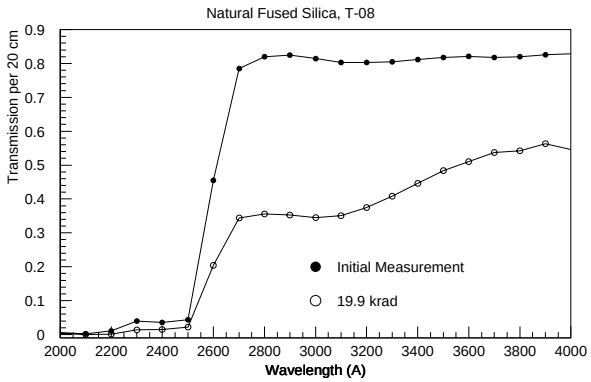

Fig. 7 Transmission as a function of wavelength of a sample of natural quartz before and after 19.9 krad irradiation. Neither measurement is corrected for losses at the quartz/air interface, so only a relative transmission measurement is possible.

Quartz Type	Manufacturer	Dose	Trans. Loss
Natural Types			
Vitrosil F	TSL [10]	7 krad	Severe
T-08	Heraeus [8]	10 krad	Very Severe
JGS3 (IR)	China	20 krad	Very Severe
Synthetic Types			
Suprasil Standard	Heraeus	280 krad	Small
JGS1 (UV)	China	650 krad	None
Spectrosil 2000	TSL	180 krad	Small
Spectrosil B	TSL	254 krad	Small

Table 1
Summary of the results of the radiation damage tests.

D. Beam Spot Distortion

In the course of measuring the reflectivity coefficient (i.e. with the internally reflected multi-bounce beam) of the Heraeus Suprasil bars, it was observed that, for about half of the bars, the laser beam spot was distorted after traversing the bars. Figure 8 shows the "lobe pattern" that was produced in these bars.

When the beam was sent through the bar such that it made a single pass through the fused silica rather than bouncing many times, a similar but simpler lobe pattern was observed. This is shown in figure 9. The opening angle between the central beam spot and lobes was typically 20 mr and the fraction of the power in the lobes was roughly estimated to be 5%. The more complicated lobe pattern observed in the multiple-bounce case is understood in terms of a superposition of many of these simple patterns, each one caused by a single pass through the fused silica.

For bars showing these lobes, a large amount of light is

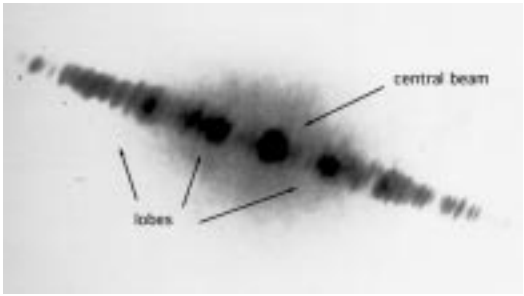

Fig. 8 Light pattern observed for lobe-producing bars.

Fig. 9 Light pattern observed in lobe-producing bars after a single pass through the bar.

scattered out of the central beam at an angle that is large with respect to expected single photon resolution of the DIRC. This effect would spoil DIRC resolution, and so it was important to develop a model for the lobe production and to examine its consequences.

III. DIFFRACTION MODEL FOR LOBE PRODUCTION

The lobes recalled the pattern that would be produced by diffraction off of a periodic grating, and so it was thought that some sort of periodic structure in the bars was likely responsible for producing the lobes. Studies of lobe-producing bars using white light also supported the idea of structure within the bars. In one of these studies, a collimated white light was shined down the length of several bars. In lobe-producing bars, the transmitted light had a non-uniform "cross-hatch" pattern [12]. In the other bars, the pattern was uniform. In another study, small samples were examined with a microscope using transmitted white light. Again, a non-uniform pattern was observed only in material that came from lobe-producing bars [12].

The structure in the ingots may be modelled as a small periodic inhomogeneity in the refractive index of the fused silica. In the simplest case, the "layers" (surfaces of constant index) of such an inhomogeneity would be planes. In general, however, the layers of inhomogeneity would be curved as shown in figure 10. In a calculation based on this model, it is found that observable diffraction occurs only when the beam is *tangent* to curved layers [13]. The opening angle (α) between

the main beam and the diffraction lobes is given by

$$\alpha = \lambda/\lambda', \tag{2}$$

where λ is the wavelength of the light and λ' is the wavelength of the inhomogeneity (the "pitch" of the "grating"), which is assumed to be sinusoidal. With $\alpha = 20\text{mr}$ and $\lambda = 6.33 \times 10^{-7}\text{m}$ (the HeNe line used in most of our studies), we find $\lambda' = 3 \times 10^{-5}\text{m}$. A calculation of the relative intensity (f) of the lobes gives [13]

$$f \approx \frac{a^2 R \lambda'}{\pi^2 \lambda^2}, \tag{3}$$

where a is the fractional amplitude of the inhomogeneity and R is the local radius of curvature of the layers. With $R = 0.05\text{m}$, $f = 0.05$ and the above values of λ and λ', we find $a = 3.7 \times 10^{-5}$. The source of the inhomogeneity is likely the manufacturing process of the raw fused silica material, so it seemed natural to study the lobes in the raw material rather than in the finished bars.

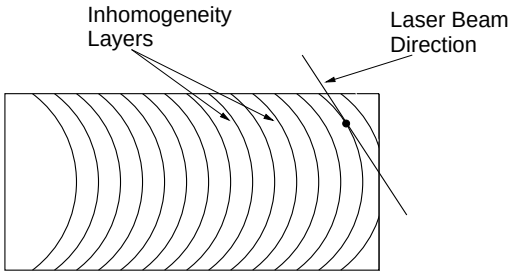

Fig. 10 Model for production of lobes off of a periodic inhomogeneity in the refraction index of fused silica. Diffraction occurs when the beam is tangent to the inhomogeneity layers, which are actually spaced much more closely than shown in the diagram.

IV. Studies of Raw Fused Silica Material

The raw fused silica material is received in the form of large cylindrical ingots, from which between 8 and 16 bars may be cut. Although the ingots are typically not well polished, and consequently scatter light on entrance and exit, it is still possible to get a beam in and out reasonably cleanly as shown in figure 11. The wedge and window were attached to the ingot using optical gel [14].

A. Lobe Production

When a HeNe laser was sent into an ingot as shown in figure 11, a lobe pattern very similar to that observed with a single pass through a bar was observed. This confirmed that it was indeed a feature of the bulk fused silica that was producing the lobes. [12]

The fraction of power in the lobes was measured by scanning a photo-diode across the pattern and recording the light intensity at each point. Figure 12 shows the results of such a scan for a sample of Heraeus Suprasil. The fraction of lobe power is found

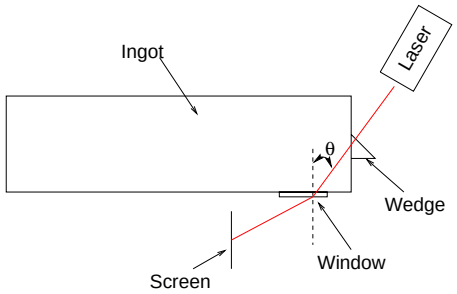

Fig. 11 Schematic of setup for observing lobes in ingots.

to be about 3% per lobe. Some samples of the other candidate material, TSL Spectrosil, also produced lobes but at a much lower power fraction — approximately 3×10^{-4}. Other samples of this material produced no observable lobes.

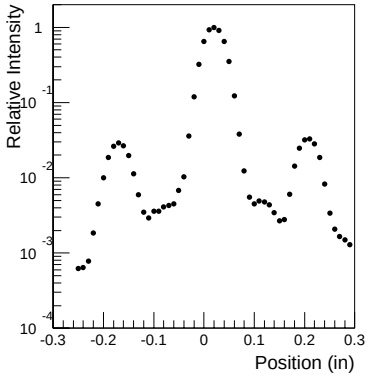

Fig. 12 Scan of the transmitted light pattern showing the lobes produced with a HeNe laser ($\lambda = 633\text{nm}$) in Heraeus Suprasil.

B. Inhomogeneity Layer Shape Measurements

Since, in our model, significant lobes are produced only at the point where the beam is tangent to the curved inhomogeneity layers, the incident angle at which lobes are produced should vary as a function of the radial position at which the beam enters the ingot. For a very thin piece of fused silica, lobes would be produced at a single angle for a given radius. For a thicker piece of fused silica, such as an ingot, or a bar, a range of radii is traversed, and so lobes are produced over a range of angles.

The model predicts an interesting phenomenon that occurs when a beam is brought into the ingot at a fixed angle and then scanned out in radius. The point-of-tangency of the beam to the layers moves forward in the ingot, as shown in figure 13. Eventually, this point comes out the front face of the ingot and lobes are no longer produced. At this "disappearance radius", the lobes "wink out" and one is left with only the central spot.

This is exactly what was observed to happen, and gives us confidence that the lobes are produced at the point of tangency between the beam and the inhomogeneity layers. Furthermore, measurement of the disappearance radius for a number of angles essentially measures the shape of the layers inside the ingot.

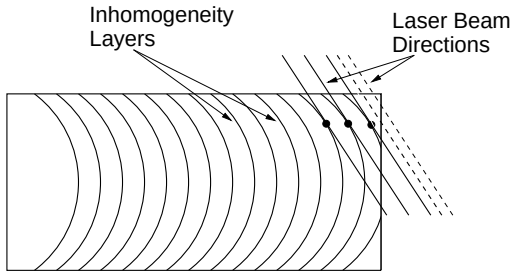

Fig. 13 Illustration of disappearance radius phenomenon. Dots on solid lines mark the point of tangency of the beam to the layers. Dashed lines represent beams that will not produce lobes since their point of tangency would lie outside the body of the ingot.

Figure 14 shows the measured disappearance radius for TSL Spectrosil and Heraeus Suprasil at a number of different angles, where θ is as defined in figure 11. Qualitatively, it is clear that the layers in TSL Spectrosil material are much nearer to normal to the ingot axis than are those of the Heraeus Suprasil sample — particularly at large radii.

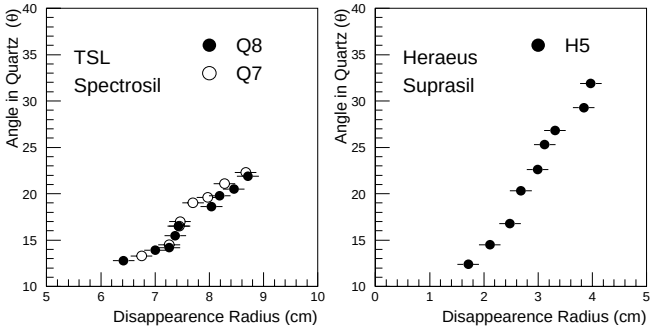

Fig. 14 Disappearance radius as a function of the angle of the beam in the fused silica for several samples of TSL Spectrosil and Heraeus Suprasil material. Lobes were not visible for angles less than about 11° in either type of material.

This is important because the disappearance radius represents the smallest radius at which light propagating at a fixed angle will produce lobes. For example, light propagating in TSL Spectrosil at an angle of 25° will not produce lobes until it gets to a radius of 9 cm. 9 cm is practically at the outer edge of a TSL ingot, and is in a region that is not used to produce bars. Furthermore, we need not concern ourselves with light that is at an angle of less than 27.5°, since in the DIRC such light is totally internally reflected at the fused silica-water interface and has no chance to be detected. We see, therefore, that TSL Spectrosil is effectively lobe-free over the whole useful radius of the ingot. Heraeus Suprasil, in contrast, has a disappearance radius of approximately 3 cm at 27.5°, well within the area of quartz that is to be cut into bars.

C. Wavelength Dependence

One further check of the tangent-to-layers model is the wavelength dependence of the lobes. The model predicts that the opening angle of the lobes should vary like

$$\theta \propto \lambda,$$

and the fraction of power in the lobes vary like

$$f \propto 1/\lambda^2.$$

These quantities were measured for beams of two different wavelengths— 633 nm and 442 nm. Table 2 shows the predicted and measured values of these quantities for the two wavelengths. The agreement is quite good and lends credence to the diffraction model.

	Predicted	Measured
$\theta_{\rm blue}/\theta_{\rm red}$	0.70	0.69 ± 0.03
$f_{\rm blue}/f_{\rm red}$	2.05	2.58 ± 0.40

Table 2
Comparison of predicted and measured values of lobe quantities.

D. Inhomogeneity Source

Synthetic fused silica ingots are produced by accreting SiO_2 vapor onto a rotating seed. Layers of approximately 20 μm are laid down with each rotation. Any spatial variation of the parameters of the accretion process (for example, a temperature gradient) could be translated into periodic variation in the refractive index of the fused silica. The 20 μm layer spacing is quite close to the inhomogeneity wavelength (λ' from section III) that is required to produce the observed opening angles. Although the inferred amplitude of the inhomogeneity is larger than expected, it seems likely that rotation of the ingot during growth plays a role in the formation of the layers.

V. CONCLUSION

An extensive program of research and development has been carried out to determine whether fused silica bars that meet the stringent requirements of the DIRC can be obtained. A number of potentially dangerous surprises have been found, such as the inadequate radiation hardness of natural fused silica and the diffraction of light due to periodic inhomogeneities. As the DIRC has passed from the R&D stage to the production stage, many of the initial tests of bar and raw material quality have been converted to quality control tests to ensure that the procured material continues to meet all of the requirements.

VI. ACKNOWLEDGEMENTS

This research is supported by the Department of Energy under contracts DE-AC03-76SF00515 (SLAC), DE-AC03-76SF00098 (LBNL), DE-AM03-76SF0010 (UCSB), and DE-FG03-93ER40788 (CSU); the National Science Foundation grants PHY-95-10439 (Rutgers) and PHY-95-11999 (Cincinnati).

VII. REFERENCES

[1] The BABAR Collaboration, "BABAR Technical Design Report," *SLAC-REP-950457, 1995*.

[2] P. Coyle et.al., "The DIRC Counter: A New Type of Particle Identification Device for B Factories," *Nucl. Instr. Methods A 343 1994* pp. 292-299.

[3] D. Aston et. al., "Test of a Conceptual Prototype of the Total Internal Reflection Cerenkov Imaging Detector (DIRC) with Cosmic Muons," *IEEE Trans.Nucl.Sci. 42 1995* pp. 534-538.
H. Staengle et. al., "Test of a Large Scale Prototype of the DIRC, a Cerenkov Imaging Detector Based on Total Internal Reflection for BABAR at PEP-II," *Nucl. Instr. Methods A 397 1997* pp. 261-282.

[4] H. Krueger, M. Schneider, R. Reif, J. Va'vra "Initial Measurements of Quartz Transmission, Internal Reflection Coefficient and the Radiation Damage," *Internal* DIRC *Note #18, October 1996*.

[5] H. Krueger, R. Reif, X. Sarazin, J. Schwiening, J. Va'vra "Measuring the Optical Quality of Quartz Bars and the Coupling of RTV to the Window," *Internal* DIRC *Note #40, May 1996*.

[6] H. Kruger, R. Reif, X. Sarazin, J. Schwiening and J. Va'vra "The Optical Scanning System for the Quartz Bar Quality Control," *Internal* DIRC *Note #54, October 1996*.

[7] Zygo Corporation, Laurel Brook Road, Middlefield, Connecticut 06455.

[8] Heraeus Amersil Inc., 3473 Satellite Blvd. 300, Duluth, Georgia 30136.

[9] J. Schwiening "Quality Control Results for Heraeus-Amersil Suprasil Bars," *Internal* DIRC *Note #82, September 1997*.

[10] TSL Group PCL, P.O. Box 6, Wallsend, Tyne & Wear, NE28 6DG, England.
Quartz Products Co., 1600 W. Lee St., Louisville, Kentucky 40201.

[11] X. Sarazin, M. Schneider, J. Schwiening, R. Reif and J. Va'vra "Radiation Damage of Synthetic Quartz and Optical Glues," *Internal* DIRC *Note #39, October 1996*.

[12] M. Convery, B. Ratcliff, J. Schwiening and J. Va'vra "Measurements of Periodic Structure in Synthetic Quartz," *Internal* DIRC *Note #87, September 1997*.

[13] S. Yellin, "Diffraction from an Oscillating Refractive Index," *Internal* DIRC *Note #75, April 1997*.

[14] Optical Gel 0607, Cargille Labs, 55 Commerce Rd., Cedar Grove, New Jersey, 07009.